Proceedings of the 4th International Conference on Mathematical Physics and Computational Simulation
DOI: 10.54254/2753-8818/2026.35667

Modeling Coverage Width of Multibeam Bathymetry and Optimizing Survey-Line Layouts for Simple Terrain

Yizhou She

Institute of Science, Shanghai University, Shanghai, China
sam_she1030@163.com

Abstract. To address the engineering problem in multibeam bathymetry that coverage width varies with terrain and fixed line spacing may cause missed sounding in shallow areas, this paper develops a three-level progressive survey-line design model consisting of single-line swath/overlap modeling, arbitrary-heading coverage correction, and global recursive line-layout optimization within a unified geometric framework. Unlike regional subdivision or dynamic-programming methods that depend mainly on cell partition or discrete state search, the proposed model gives an explicit geometric chain from depth and slope to line spacing. Sensitivity tests for slope, opening angle, and overlap threshold, together with a measured-terrain checking procedure, are added to clarify robustness and engineering applicability. A numerical example shows that, when the sea area is 4 nautical miles long from east to west and 2 nautical miles wide from north to south, with a central depth of 110 m, a slope of 1.5°, and a transducer opening angle of 120°, the optimal lines should be arranged parallel to isobaths. The solution requires 34 survey lines and a total length of about 125.94 km. The results provide a concise and implementable basis for efficient bathymetric operation over regular sloping seabeds.

Keywords: multibeam bathymetry, coverage width, overlap rate, survey-line layout, simple terrain

1. Introduction

A multibeam bathymetric system can form multiple acoustic beams simultaneously in the cross-track direction. Compared with a single-beam system, it offers higher coverage efficiency and finer terrain-resolution capability, and it has been widely used in channel maintenance, bridge-pier scour and siltation detection, and hydraulic-engineering surveys [1-3], as well as unmanned-vessel bathymetric mapping [4, 5]. In practical operations, the swath coverage width is controlled not only by the transducer opening angle but also by seabed slope, survey-line direction, and local water depth. If a fixed line spacing is adopted directly, excessive overlap in deeper water and insufficient coverage in shallower water may occur at the same time, weakening both survey efficiency and data completeness. Therefore, a reliable coverage model is an important prerequisite for both safety and economy in survey design.

Existing studies have discussed the calculation of coverage width and overlap rate from geometric relationships [6, 7], and have proposed survey-line layout approaches for simple slopes or regular sea areas [8-10]. Related work also extends line planning through multidimensional structure analysis and multimodal clustering [11, 12]. For complex terrain, regional subdivision, traversal search, and

© 2026 The Authors. This is an open access article distributed under the terms of the Creative Commons Attribution License 4.0 (https://creativecommons.org/licenses/by/4.0/).

DOI: 10.54254/2753-8818/2026.35667

dynamic programming have been investigated [13-15]. Compared with regional-subdivision methods, the present method does not first divide the whole sea area into many independent cells; compared with dynamic programming, it does not treat line positions mainly as a discrete state-search problem. Its innovation is to use one geometric framework to connect swath width, heading effect, and recursive line placement, thereby giving an interpretable closed-form planning rule for regular single-slope seabeds.

On this basis, this paper focuses on three core problems in multibeam bathymetry. First, it establishes a coverage-width and overlap-rate model for lines arranged along isobaths. Second, it constructs a coverage-width model under an arbitrary survey-line direction. Third, under simple-terrain conditions, it develops a shortest-line layout method that satisfies full coverage and overlap-rate constraints. While retaining key conclusions and core formulas, the paper emphasizes engineering usability and interpretability of the results. The three problems are not independent; rather, they correspond to different levels of the same planning task. The first model describes the basic coverage mechanism, the second model extends it to directional sailing, and the third model uses the previous results to determine actual line positions. This arrangement helps avoid treating line spacing as an empirical constant and instead links it directly to seabed geometry.

2. Coverage width and overlap model along isobaths

As shown in Figure 1, a single planar sloping seabed is considered. Let the opening angle of the multibeam transducer be θ, the seabed slope be α, and the water depth at the center of the sea area be h_0. This assumption simplifies the seabed into a regular geometric surface, but it still preserves the most important depth-changing feature that affects multibeam coverage. It is therefore suitable for deriving clear analytical relationships before more complex terrain is considered.

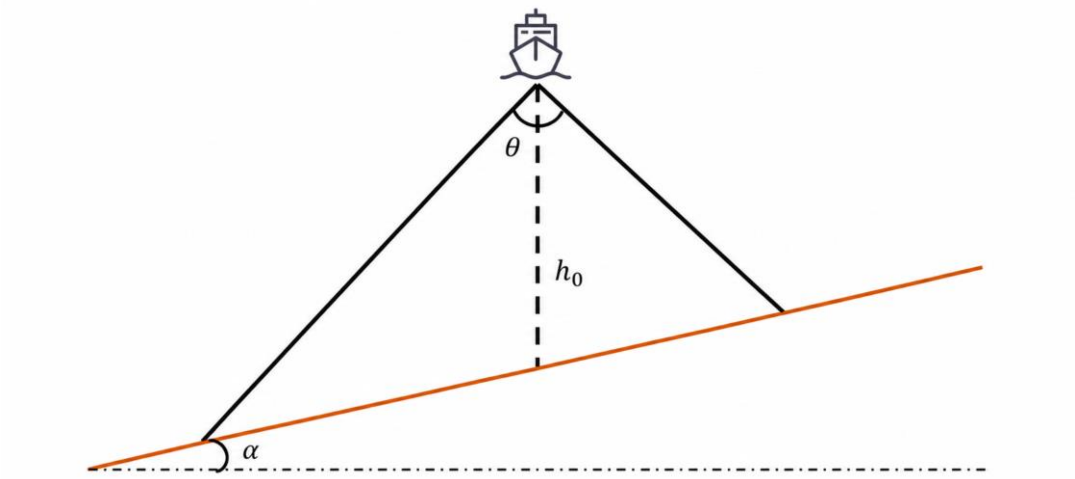


Figure 1. Schematic diagram of coverage width

When survey lines are arranged parallel to isobaths, let x denote the cross-track offset of a line center relative to the center of the sea area. Here, $x > 0$ means movement toward the shallow side, whereas $x < 0$ means movement toward the deep side. The local water depth can then be written as

$$h(x) = h_0 - x\tan\alpha \tag{1}$$

Let the half-swath widths toward the deep side and the shallow side be $a(x)$ and $b(x)$, respectively. From the geometric relationship between the fan-shaped beam and the sloping seabed, one obtains

DOI: 10.54254/2753-8818/2026.35667

$$a(x) = \frac{h(x)\sin(\theta/2)}{\cos(\theta/2+\alpha)}, \qquad b(x) = \frac{h(x)\sin(\theta/2)}{\cos(\theta/2-\alpha)} \tag{2}$$

Therefore, the total coverage width of a single line on the slope is

$$W(x) = a(x) + b(x) \tag{3}$$

As shown in Figure 2, if the center positions of two adjacent survey lines are x_i and x_{i+1}, and their horizontal spacing is $d_i = x_{i+1} - x_i$, the overlap rate of the two adjacent swaths can be expressed as

$$\eta_i = \frac{a(x_{i+1}) + b(x_i) - d_i/\cos\alpha}{W(x_i)} \tag{4}$$

Here, η_i <0 indicates that a missed-sounding gap has already appeared between the two adjacent swaths. The model shows that coverage width varies linearly and positively with local water depth, whereas the overlap rate is jointly controlled by depth variation and survey-line spacing. In other words, a larger depth expands the acoustic footprint on the seabed, while a smaller depth compresses it. If the spacing remains unchanged, this compression first reduces redundant overlap and then produces gaps. The sign and magnitude of the overlap rate therefore provide an intuitive criterion for judging whether a line plan is conservative, efficient, or insufficient. Under the isobath-parallel arrangement, the survey vessel sails along a direction in which the depth of the line center is approximately unchanged during a single pass. The main depth difference then appears between neighboring lines rather than along one line, which makes the overlap relationship easier to describe and compare.

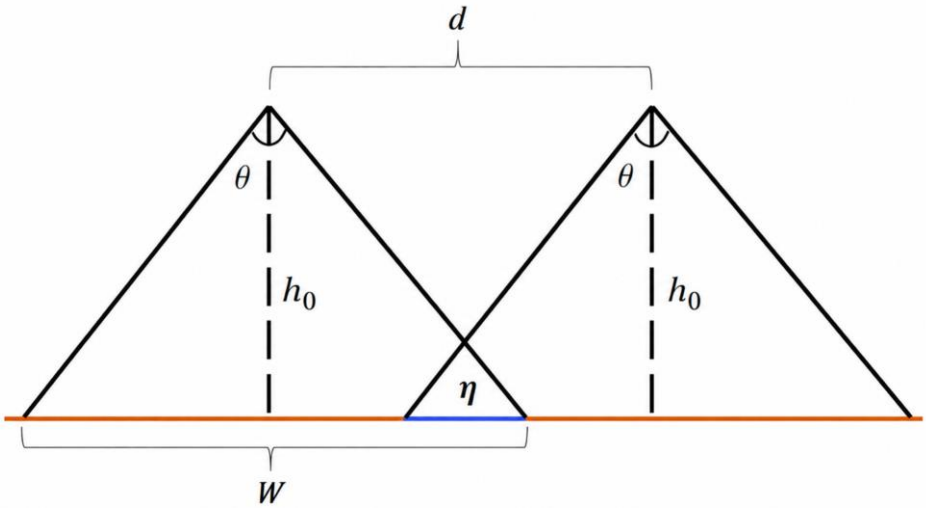


Figure 2. Relationship among adjacent swath width, line spacing, and overlap rate

To verify the model, the transducer opening angle is set to $\theta = 120°$, the slope to $\alpha = 1.5°$, the center water depth to $h_0 = 70$ m, and the spacing between adjacent survey lines to a constant 200 m. The calculation results are shown in Table 1. This example uses a constant spacing in order to show the limitation of a simple uniform-line strategy. Since all other parameters are fixed, the changes in coverage width and overlap rate can be attributed directly to the depth variation caused by the sloping seabed.

DOI: 10.54254/2753-8818/2026.35667

Table 1. Coverage width and overlap-rate results for Model 1

Distance from center / m	Water depth / m	Coverage width / m	Overlap with previous line / %
-800	90.95	315.81	—
-600	85.71	297.63	33.64
-400	80.47	279.44	29.59
-200	75.24	261.26	25.00
0	70.00	243.88	19.78
200	64.76	224.70	13.18
400	59.53	206.00	6.80
600	54.29	188.51	-1.39
800	49.05	170.32	-11.17

Table 1 shows that, as the survey line moves toward the shallow area, water depth decreases continuously and the coverage width decreases accordingly. Under fixed spacing, the overlap rate decreases from a relatively large positive value in the deep-water area to a negative value, indicating that the shallow area is the first place where missed sounding occurs. This result explains the engineering rule that lines can be relatively sparse in deep water but must be densified in shallow water. It also provides a basis for the subsequent optimization of survey-line direction and position. The numerical trend also indicates that evaluating only an average water depth is not enough for a sloping area. A spacing that appears acceptable near the center may be too large on the shallow side, while a spacing designed for the shallow side may become overly conservative in deep water. Thus, line spacing should preferably be adjusted according to local coverage width or generated through a recursive layout procedure.

3. Coverage width model for an arbitrary survey-line direction

The case in which the survey line is no longer parallel to the isobaths is considered next. As shown in Figure 3, let β be the angle between the survey-line direction and the direction from shallow to deep water, and let s be the sailing distance of the survey vessel along the survey line relative to the center of the sea area. According to the geometric relationship, the water-depth variation along this direction can be expressed as

$$h(\beta, s) = h_0 + s\cos\beta\tan\alpha \tag{5}$$

At the same time, the effective slope angle in the operating profile is no longer equal to the original seabed slope but depends on the survey-line direction. Let the equivalent slope angle in the profile be $\gamma(\beta)$. Then

$$\gamma(\beta) = \arctan\left(|\sin\beta|\tan\alpha\right) \tag{6}$$

Thus, the two half-swath widths under an arbitrary direction can be written uniformly as

$$a(\beta, s) = \frac{h(\beta,s)\sin(\theta/2)}{\cos\left(\theta/2+\gamma(\beta)\right)}, \qquad b(\beta, s) = \frac{h(\beta,s)\sin(\theta/2)}{\cos\left(\theta/2-\gamma(\beta)\right)} \tag{7}$$

Accordingly, the total coverage width satisfies

$$W(\beta, s) = a(\beta, s) + b(\beta, s) \tag{8}$$

DOI: 10.54254/2753-8818/2026.35667

This expression incorporates both along-track depth variation and profile slope variation into the same model. When the former effect dominates, coverage width increases more clearly as the survey line advances toward deeper water. When along-track depth variation tends to zero, coverage width is mainly determined by the local profile slope. Therefore, the arbitrary-direction model can be understood as a correction to the isobath-parallel model. It retains the same geometric basis but adds two directional effects: the depth of the vessel changes along the sailing path, and the cross-track section intercepted by the beam has a different slope. These two effects may reinforce or offset each other depending on the value of the direction angle. This situation is common when the boundary of a survey area, navigation restrictions, or operational convenience requires a heading that differs from the isobath direction. Once the heading changes, the vessel may move partly toward deeper water or partly toward shallower water while it is collecting data. This equivalent slope describes the slope actually observed in the cross-track profile of the multibeam fan; even if the physical seabed slope is fixed, the profile cut by the acoustic fan changes with the heading, so the apparent slope controlling the two half-swath widths also changes.

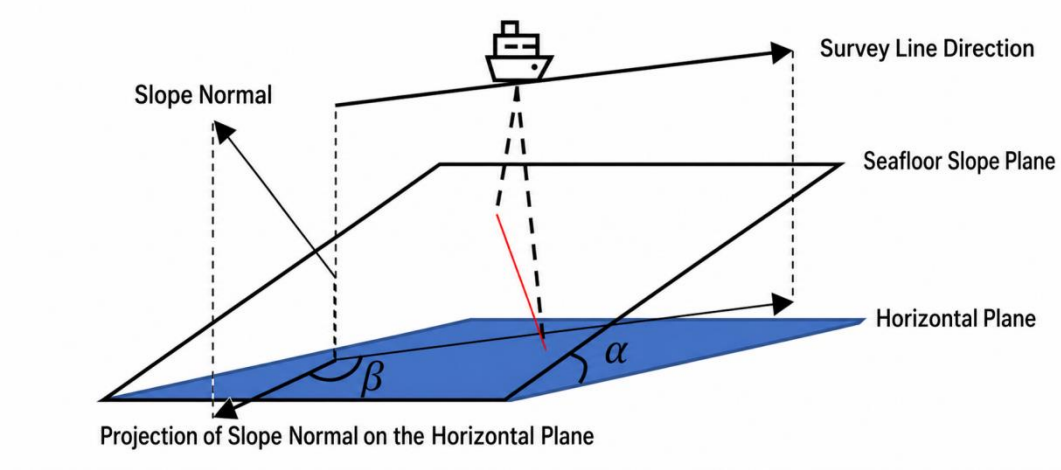


Figure 3. Geometric relationship under an arbitrary survey-line direction

Taking $\theta = 120°$、$\alpha = 1.5°$, $h_0 = 120$ m, and $s = 0 - 2.1$ nautical miles, the coverage-width results in Table 2 are obtained.

Table 2. Coverage-width results for Model 2

Coverage width / m		Distance from the survey vessel to the central point of the sea area / nautical miles							
		0	0.3	0.6	0.9	1.2	1.5	1.8	2.1
Angle between survey line directions / °	0	415.692	466.091	516.490	566.889	617.288	667.686	718.085	768.484
	45	416.192	451.872	487.552	523.232	558.912	594.592	630.273	665.953
	90	416.692	416.692	416.692	416.692	416.692	416.692	416.692	416.692
	135	416.192	380.511	344.831	309.151	273.471	237.791	202.110	166.430
	180	415.692	365.293	314.894	264.496	214.097	163.697	113.299	62.900
	225	416.192	380.511	344.831	309.151	273.471	237.791	202.110	166.430
	270	416.692	416.692	416.692	416.692	416.692	416.692	416.692	416.692
	315	416.192	451.872	487.552	523.232	558.912	594.592	630.273	665.953

Table 2 leads to the following observations. When $\beta = 90°$ or $270°$, the survey line extends along an isobath, the along-track water depth remains unchanged, and the coverage width is constant at

DOI: 10.54254/2753-8818/2026.35667

416.692 m. When $\beta = 0°$, the survey line always advances toward deeper water; as s increases from 0 to 2.1 nautical miles, the coverage width increases from 415.692 m to 768.484 m. When $\beta = 180°$, the survey line advances toward shallower water and the coverage width decreases to 62.900 m. Therefore, the direction angle does not merely affect local geometry; it directly determines the evolution trend of swath width during operations. The symmetry of the table is also consistent with the physical meaning of the direction angle. Headings that differ by the same angle from the isobath direction produce similar equivalent profile slopes, while headings pointing toward opposite depth directions produce opposite depth-change trends. This comparison makes clear why the direction parallel to the isobaths is attractive for simple terrain: it keeps the swath width nearly stable, reduces the need for frequent spacing adjustment along a single line, and simplifies the subsequent layout calculation.

4. Optimal survey-line layout model for simple terrain

Consider a rectangular sea area to be surveyed, with east-west length L and north-south width W. The seabed is a single slope that is deeper in the west and shallower in the east. To minimize the total survey-line length, the optimal survey-line direction must first be determined. Suppose that a trial survey line of length 2l is arranged from the sea-area center along direction angle β. The corresponding swath coverage area can be expressed as

$$F(\beta) = \int_{-l}^{l} W(\beta, s)\, \mathrm{d}s \tag{9}$$

When l=100 m and β is traversed numerically, Figure 4 shows that F(β) reaches its maximum at β=90°, which means that the seabed area covered per unit survey-line length is largest when the survey line is parallel to the isobaths. Geometrically, the isobath-parallel heading makes the depth-gradient vector perpendicular to the track, so the line center depth remains constant along the whole pass and the unit sailing length is converted into a stable swath. A slope-parallel or oblique heading contains both shallow and deep segments in the same pass; the shallow segment narrows the effective swath and boundary truncation increases, so the average covered area per unit line length is smaller.

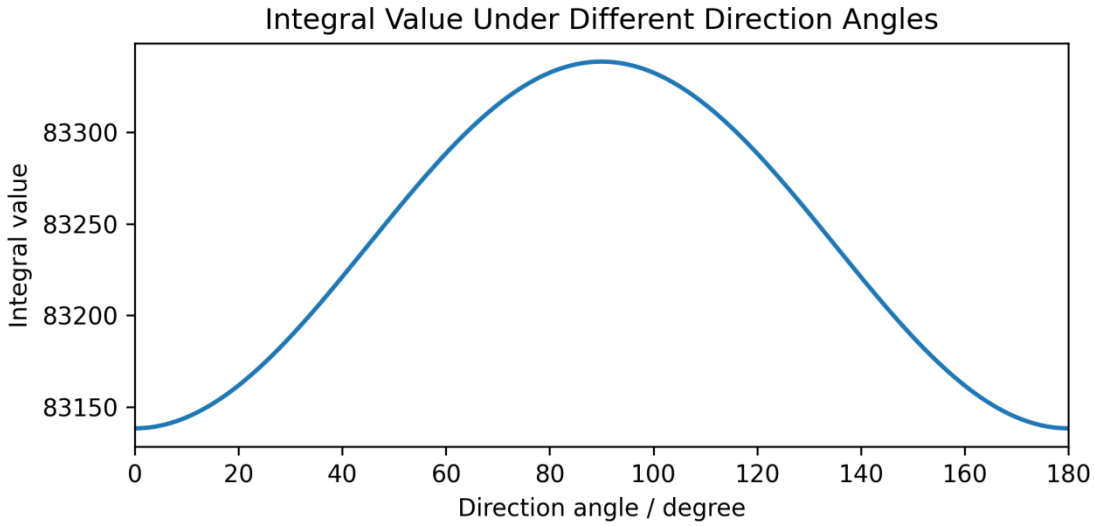


Figure 4. Numerical results of unit-line coverage area under different direction angles

After the optimal direction has been determined, let the transverse coordinate $x \in [0, L]$ point from the eastern boundary to the western boundary, and let the water depth at the eastern boundary be

DOI: 10.54254/2753-8818/2026.35667

$$h_E = h_0 - \frac{L}{2}\tan\alpha \tag{10}$$

so that the water depth at the n-th survey-line position is $h(x_n) = h_E + x_n\tan\alpha$. To minimize the number of lines while satisfying full coverage, the overlap rate between adjacent swaths is fixed at the lower bound of the allowable range, namely

$$\eta\left(x_n, x_{n+1}\right) = 0.1, \qquad n = 1,2, \ldots, N-1 \tag{11}$$

The 10% lower bound is used as an illustrative engineering safety margin rather than a universal constant: a larger value improves tolerance to positioning, attitude, and sounding errors but increases line number and total length, whereas a smaller value improves efficiency but reduces robustness.

At the same time, to ensure that both lateral boundaries of the sea area are covered, the first and last survey lines should satisfy

$$x_1 - b\left(x_1\right)\cos\alpha \le 0 \tag{12}$$

$$x_N + a(x_N)\cos\alpha \ge L \tag{13}$$

These conditions define a recursive layout method from the shallow side toward the deep side. $\eta_{\min}$ is the allowable lower overlap bound; The first line is selected so that its shallow-side edge just covers the eastern boundary; subsequent lines are solved sequentially by $\eta_{\min}$=10%; and the recursion terminates only when the deep-side edge of the last line reaches or exceeds the western boundary. This termination rule gives an unambiguous and reproducible full-coverage criterion. If all lines are parallel to isobaths, each survey line has length W, and the total length is therefore

$$L_{\text{tot}} = NW \tag{14}$$

Taking L=4 nautical miles (7408 m), W=2 nautical miles (3704 m), h_0=110 m, α=1.5°, θ=120°, and $\eta_{\min}$=10%, the optimal direction is parallel to the isobaths. All nautical-mile quantities are converted to meters before the recursive calculation. The resulting survey-line layout is shown in Table 3. Starting from the shallow boundary is reasonable because the shallow side has the smallest coverage width and is most likely to suffer from missed sounding.

Table 3. Optimal survey-line positions for simple terrain

1	2	3	4	5	6	7	8	9
358.521	947.861	1491.175	1992.058	2453.823	2879.525	3271.981	3633.787	3967.337
10	11	12	13	14	15	16	17	18
4274.837	4558.323	4819.669	5060.604	5282.723	5487.495	5676.275	5850.321	6010.757
19	20	21	22	23	24	25	26	27
6158.671	6295.034	6420.747	6536.643	6643.487	6741.987	6832.794	6916.510	6993.687
28	29	30	31	32	33	34		
7064.837	7130.431	7190.902	7246.650	7298.044	7345.425	7389.105		

Note: In each pair of rows, the upper row gives the survey-line number and the lower row gives the cross-track coordinate x in meters.

The visualization of the survey-line distribution is shown in Figure 5.

DOI: 10.54254/2753-8818/2026.35667

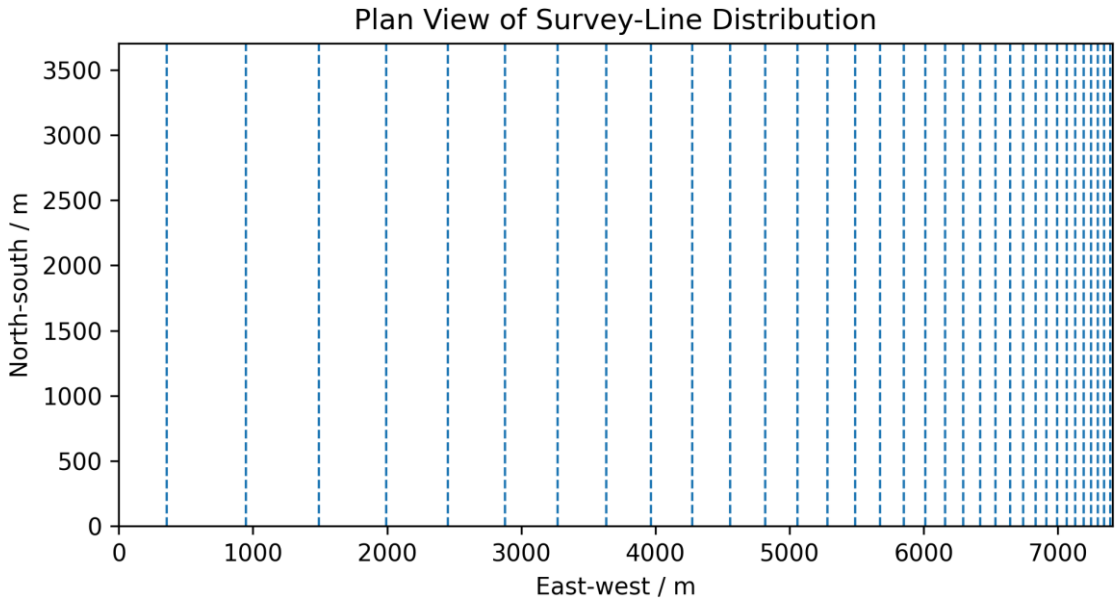


Figure 5. Optimal survey-line layout for simple terrain

Figure 5 indicates that the spacing between survey lines gradually increases from east to west. The reason is that the coverage width is smaller in the shallow eastern area, so lines must be densified to avoid missed sounding. In contrast, the coverage width is larger in the deeper western area, and retaining small spacing would produce obvious redundant overlap. The resulting layout satisfies the full-coverage requirement while keeping the number of survey lines relatively low, demonstrating the engineering effectiveness of the model. From an operational perspective, this pattern is also convenient because it provides a clear rule for field planning: the vessel should perform more closely spaced passes near the shallow boundary and may gradually relax the spacing when moving toward deeper water. The layout therefore avoids both of the common problems in uniform designs, namely shallow-water gaps and deep-water redundancy. It also shows that the optimization result is not an abstract numerical outcome but a line arrangement that matches practical bathymetric experience.

Scope and applicability statement: the single-slope terrain is used as a controllable benchmark for verifying the geometric mechanism. In actual surveys, terrain undulation, sounding noise, sound-speed residuals, and roll/pitch/heave errors should be handled by local plane fitting, regional subdivision, and a larger $\eta_{\min}$ safety allowance. The purpose of this example is analytical model validation rather than a full ranking of dynamic-programming or subdivision algorithms; those algorithms are more suitable for complex terrain after discretization, while the present model provides the local geometric rule used to set spacing inside each simple-slope cell. Sensitivity is monotonic: increasing $\eta_{\min}$ or strengthening the termination margin increases the number and total length of lines, whereas decreasing them improves efficiency but weakens robustness.

Sensitivity and measured-terrain verification: keeping the area size and h_0 unchanged, one-factor tests give Table 4. The results are monotonic: a steeper slope, a smaller opening angle, or a larger $\eta_{\min}$ increases the required line number and total length. For field verification, measured depth $h_m(\mathrm{x})$ can replace the planar depth h(x), and local slope $\alpha_m(x)$ can be obtained by moving-window plane fitting. The planned lines are then checked by recalculating W_i and η_i on the measured profile and confirming that min $\eta_i \geq 0$ and both boundaries remain covered.

DOI: 10.54254/2753-8818/2026.35667

Table 4. One-factor sensitivity results and measured-terrain checking rule

Tested factor	Values or checking item	N / L_{tot}	Engineering implication
Slope α	0.5° / 1.0° / 1.5°	23 / 85.19 km; 25 / 92.60 km; 34 / 125.94 km	Steeper slopes reduce shallow-side coverage and require more lines.
Opening angle θ	100° / 120° / 140°	50 / 185.20 km; 34 / 125.94 km; 22 / 81.49 km	A wider fan angle expands coverage and shortens the plan.
Overlap η_{min}	5% / 10% / 20%	33 / 122.23 km; 34 / 125.94 km; 39 / 144.46 km	Higher overlap improves robustness but increases cost.
Measured terrain	$h_m(x)$, $\alpha_m(x)$ from local fitting	Report min η_i, boundary gap, and line-offset RMS	Checks whether the planar-cell assumption is acceptable.

5. Conclusions

This paper establishes a three-level progressive model for multibeam survey-line design over a regular single-slope seabed. Compared with cell-based subdivision and discrete dynamic programming, the method derives spacing from an explicit geometric overlap relation, so each result can be traced to depth, slope, opening angle, and the overlap threshold.

Level 1 shows that coverage width increases with water depth; under fixed spacing, shallow areas first lose sufficient overlap. Level 2 shows that arbitrary headings change both along-track depth and equivalent profile slope. Therefore, the isobath-parallel direction is preferred for simple slopes when navigation constraints do not dominate.

Level 3 converts the geometric model into a recursive line-layout rule. In the example, 34 survey lines are required and the total length is about 125.94 km. Sensitivity analysis confirms that the plan becomes more conservative when the slope or overlap threshold increases, and more efficient when the opening angle increases.

The model is applicable when each planning cell can be approximated by a plane and when positioning, attitude, sound-speed, and depth errors are absorbed by η_min. For complex terrain, the area should be divided by local plane fitting, the present model applied in each cell, and the overlap margin enlarged according to engineering error estimates. Future work should benchmark the method on measured bathymetric grids against regional-subdivision and dynamic-programming algorithms.

References

[1] Wang, X., Hu, S., & Lu, Y. (2024). Brief analysis of the application of the NORBIT iWBMS integrated multibeam bathymetric system in rapid channel survey. *China Water Transport, 3*, 42–45. (in Chinese)

[2] Chen, X. (2024). Application of a multibeam bathymetric system combined with three-dimensional imaging sonar in bridge-pier scour and siltation detection. *Value Engineering, 43*(5), 124–126. (in Chinese)

[3] Li, M., & Liang, D. (2023). Application of multibeam bathymetric systems in water conservancy engineering. *Guangxi Water Resources & Hydropower Engineering, 6*, 9–14. (in Chinese)

[4] Liu, D. (2024). Application of unmanned-vessel multibeam bathymetric technology in evaluation of riprap bank-protection engineering. *Guangdong Water Resources and Hydropower, 1*, 93–96, 105. (in Chinese)

[5] Sha, H., Fei, X., Ye, F., et al. (2022). Application of an acoustic-inertial integrated single-beam bathymetric system in Yangtze River channel surveys. *Bulletin of Surveying and Mapping, 9*, 162–166. (in Chinese)

DOI: 10.54254/2753-8818/2026.35667

[6] Wang, N., Huang, J., & Rao, T. (2023). Optimization model of survey lines under a multibeam bathymetric system. *Electroacoustic Technology, 47*(6), 61–64. (in Chinese)
[7] Xia, H., Qiu, S., Shan, X., et al. (2024). Simulation optimization of multibeam survey lines. *Technology Wind, 5*, 61–63. (in Chinese)
[8] Wang, Z. (2024). Research on the problem of multi-beam line measurement based on the cattle plowing traversal algorithm. *Highlights in Science, Engineering and Technology, 82*, 10–18.
[9] Guo, Q., Fu, C., Chen, Y., et al. (2023). Application of multi-beam bathymetry system in shallow water area. *Journal of Physics: Conference Series, 2428*(1), Article 012042.
[10] Suo, J., Zhu, H., & Sun, W. (2023). Study on multi-beam line measurement problem based on geometric mathematical model. *Academic Journal of Science and Technology, 8*(1), 18–24.
[11] Zhan, H., & Ma, Y. (2023). Research on multi-beam survey line based on multi-dimensional structure analysis. *Highlights in Science, Engineering and Technology, 75*, 344–352.
[12] Liu, J., He, H., & Li, M. (2024). Research on the optimization of multibeam bathymetric survey line arrangement based on multimodal and clustering techniques. *Highlights in Science, Engineering and Technology, 88*, 16–28.
[13] Gao, Z., Hou, Y., Huang, W., et al. (2024). Survey-line design based on the main-objective method. *Mathematical Modeling and Its Applications, 13*(1), 96–101. (in Chinese)
[14] Sun, D., Deng, Y., & Zhu, S. (2023). Multibeam bathymetric model based on gridding and traversal search algorithms. *Journal of Nantong Vocational University, 37*(4), 70–76. (in Chinese)
[15] Wang, N., Yu, Z., & Wang, J. (2023). Multibeam survey-line layout model based on dynamic programming. *Journal of Nantong Vocational University, 37*(4), 64–69, 97. (in Chinese)